

# Irreversibility of the pressure-induced phase transition of quartz and the relation between three hypothetical post-quartz phases

Carlos Campaña and Martin H. Müser

*Department of Applied Mathematics, University of Western Ontario, London, Ontario N6A 5B7, Canada*

John S. Tse

*Steacie Institute for Molecular Sciences, National Research Council of Canada, Ottawa, Ontario K1A 0R6, Canada*

Daniel Herzbach and Philipp Schöffel

*Institut für Physik, WA 331, Johannes Gutenberg-Universität, 55099 Mainz, Germany*

(Received 9 June 2004; published 1 December 2004)

Our atomistic computer simulations mainly based on classical force fields suggest that the pressure-induced transition from  $\alpha$  quartz to quartz II at 21 GPa is irreversible. While quartz II is ferroelastic in principle, the transition itself is coelastic, as the shape of the newly formed crystal is determined by the handedness of  $\alpha$ -quartz. Upon releasing the pressure, our model quartz II remains stable down to 5 GPa, where it undergoes an isosymmetric transformation into a less dense polymorph. If the classical force field model of quartz II is compressed quickly to 50 GPa, a yet different post-quartz polymorph results, which can probably best be described as an incommensurate modulation of the quartz II structure. We discuss the equation of state and the thermomechanical stability of all four phases. One of the post-quartz phases can be switched elastically by shear between two symmetrically equivalent shapes; however,  $\alpha$ -quartz appears as an intermittent phase.

DOI: 10.1103/PhysRevB.70.224101

PACS number(s): 61.50.Ks, 81.30.Hd

## I. INTRODUCTION

$\alpha$ -quartz (also called low quartz and quartz I) is the most stable silica ( $\text{SiO}_2$ ) polymorph at ambient conditions. It becomes unstable when subjected to large external pressures  $P$ .<sup>1-3</sup> When  $P$  is increased quickly at room temperature, quartz I transforms into a disordered solid at about 22 GPa. However, when  $P$  is increased sufficiently slowly, quartz I transforms into a new crystalline phase called quartz II. This transition also occurs at a pressure  $P_{I \rightarrow II}(T=300\text{K}) \approx 22$  GPa.<sup>4,5</sup>

Due to silica's commercial applications and its abundance in nature, there is a lot of interest in understanding the properties and the phase transformations of silica in general and of quartz in particular. Concerning the pressure-induced phase transformation, there are at least three unsettled questions. (i) What is the mechanism that drives the transition from  $\alpha$ -quartz to quartz II and is the transition ferroelastic? (ii) Does quartz II convert back to  $\alpha$ -quartz when the pressure is released? (iii) What is the relation between the recently identified metastable post-quartz<sup>6</sup> and quartz I and II? Before presenting our computational methods and results, we will discuss these three issues in more detail.

Issue (i): The pressure-induced instability of  $\alpha$ -quartz and its concurrent densification was predicted theoretically<sup>1,2</sup> and observed experimentally<sup>3,4</sup> a little more than a decade ago. The theoretical analysis suggested that the elastic constants of  $\alpha$ -quartz become soft as  $P_{I \rightarrow II}$  is approached. However, it was concluded that the transition is driven by an instability at the  $K$  point, which is not in the center of the Brillouin zone.<sup>2</sup> The microscopic parameters driving such transitions can soften the acoustic modes with which they are associated, but not necessarily up to zero.<sup>7</sup> While the onset of instability

at the  $K$  point seems established, the extent with which quartz softens has been a matter of a recent controversy.<sup>8-10</sup> Experiments<sup>8</sup> found that quartz softens considerably less with increasing pressure than predicted theoretically. However, it was argued that the discrepancy between experiment and simulation were due to an inconsistent use of stability criteria.<sup>9</sup> The determination of mechanical stability is a subtle issue at nonzero stresses, because the definition of elastic constants is not unique in that case.<sup>11,12</sup>

Another conclusion of Ref. 8 was challenged: namely, the classification of the pressure-induced phase transformation as ferroelastic.<sup>13</sup> A crystal is called ferroelastic when it is able to switch its shape if a sufficiently large elastic force is applied to it. This implies broken symmetry related to a spontaneous distortion of the crystal analogous to a ferromagnet's spontaneous magnetization. However, it may well be that the  $I \rightarrow II$  transition itself is not involved in the symmetry breaking. In that case, there would be a shape change associated with the transition *without* shape-related symmetry breaking. Consequently, the phase transformation would have to be classified as coelastic.<sup>14</sup>

Issue (ii) arises from electron diffraction patterns of decompressed quartz II.<sup>4</sup> In their work, Kingma *et al.* reported that "...the high-pressure phase reverts to quartz or a quartz like material, upon decompression. Faint, yet distinct non-quartz intensities are detected along various reciprocal lattice directions between primary quartz spots...." The analysis of Raman spectra of decompressed quartz led the authors to conclude that *a decompression transition from the new crystalline phase to a twinned quartzlike structure occurs.*<sup>4</sup> The true structure remains yet to be determined.

Question (iii) is related to issue (ii). Haines *et al.*<sup>6</sup> identified a new stable silica polymorph after decompressing a

sample from 45 GPa to ambient conditions. The high-pressure sample was obtained from shock-compressing quartz II. Moreover, one year before those experiments, one of the present article's authors<sup>15</sup> found evidence for a new post-quartz phase resulting from decompressing quartz II. However, these results have not yet been supported by *ab initio* calculations.

In this paper, we intend to address these three central questions. For this purpose, we employ molecular dynamics (MD) simulations based on the model potential suggested by van Beest, Kramer, and van Santen<sup>16</sup> (BKS). Some results will be checked with an alternative model potential developed recently by Tangney and Scandolo,<sup>17</sup> as well as by *ab initio* calculations.

## II. METHODS

The BKS potential is one of the model potentials<sup>18,19</sup> that have proved particularly useful in simulating various silica polymorphs in general<sup>20</sup> and elastic properties—for example at the transition between  $\alpha$ - and  $\beta$ -quartz, in particular.<sup>21</sup> Anharmonic effects at low temperatures,<sup>22</sup> pressure-induced distortion of  $\text{SiO}_4$  tetrahedral units in  $\alpha$ -quartz under pressure,<sup>5</sup> and the properties of disordered silica melts<sup>23</sup> are also reproduced reasonably well with the BKS potential.

Unless noted otherwise, all MD simulations are performed at room temperature and at constant external, isotropic stress, which means that shape and size of the simulation cell are variable. Initial configurations consist of single crystals of  $\alpha$ -quartz composed of 720  $\text{SiO}_2$  units. One initial configuration corresponded to left-handed  $\alpha$ -quartz, the other initial configuration to right-handed  $\alpha$ -quartz. The crystal axis at zero pressure corresponds to  $a$ ,  $b$ , and  $c \approx 29.8$ ,  $34.5$ , and  $27.3$  Å, respectively. Time steps are 1 fs long, and 10 000 steps are usually discarded for equilibration. Here 50 000 time steps are retained for observation. The equations of motion were thermostated using a Langevin thermostat with coupling  $\gamma=4$  THz. This limits the resolution of dynamical data to a little less than  $\delta\nu \approx 1$  THz.

The Parrinello-Rahman method was used for the box dynamics.<sup>24</sup> We ensured good thermal averages of the strain fluctuations by coupling the geometry of the cell to a stochastic thermostat  $\gamma_{\text{box}}$  of a slightly smaller value than that for the particles—to be specific, typically  $\gamma_{\text{box}} \approx \gamma/2$ . The box inertia  $W$  was chosen small—i.e., so small that the fluctuations of the box shape occurred on time scale barely larger than those of the particles. A similar procedure resulted in excellent values for elastic constants of  $\alpha$  and  $\beta$  quartz in previous work.<sup>21</sup> We want to point out at this point that choosing small box inertia  $W$  was important to invoke the pressure-induced crystal-crystal transitions. Large values of  $W$  slow down the dynamics with respect to the real dynamics. Large value of  $W$  turned out to favor amorphization of the  $\text{SiO}_2$  over the pressure-induced crystal-crystal transition.

Thermal averages in general and elastic constants are evaluated on the basis of 100 000 time steps. Before crossing a phase transition point, one system is replicated 10 times, equilibrated 60 000 time steps with different random seeds for the Langevin thermostat, before the transition was in-

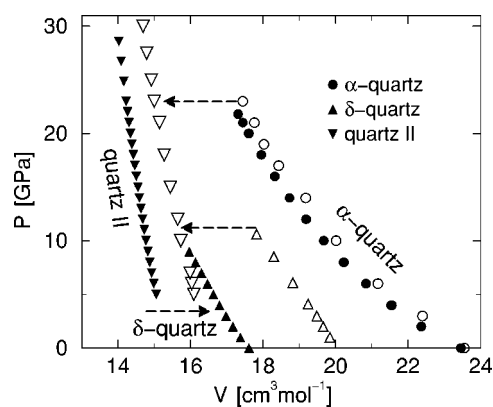


FIG. 1. Equation of state at room temperature for three quartz species. The arrows mark possible phase transformation paths. Dashed lines are drawn to guide the eye. Open symbols are results from *ab initio* simulations.

voke via a small pressure change. We run this number of replica to (statistically) explore the effect of handedness on the shape of the new pressure-induced crystalline phase.

We also rerun some of our simulations with an alternative force field that was recently developed by Tangney and Scandolo<sup>17</sup> (TS). The TS potential does not only contain two-body interactions, but it also includes inducible dipoles on the oxygen atoms and thus has the ability to incorporate effectively many-body effects. A detailed study of the TS potential will be presented elsewhere.<sup>25</sup> At this point, we may comment that the TS potential gives excellent agreement with experimental data for all quantities and phases that were tested.

Last, *ab initio* calculations using the VASP code<sup>26</sup> were employed in order to ensure the reliability of our conclusions. Full geometry optimizations were made of the MD-predicted unit cell structures. The projected-augmented-wave (PAW) pseudopotentials<sup>27</sup> provided in the library for Si and O were used in these calculations.

## III. RESULTS

### A. Phase transformations and equation of state

The equation of state resulting from the simulations are shown in Fig. 1. We start at  $P=0$  GPa with an ideal  $\alpha$ -quartz configuration, increase  $P$  gradually to 28 GPa, and go back to zero pressure. On increasing pressure,  $\alpha$ -quartz transforms into quartz II at  $P=21.7$  GPa, in agreement with experimental observations<sup>4</sup> and previous molecular dynamics simulation studies.<sup>28,29</sup> An interesting observation is that the shape of the quartz II simulation cell is predetermined by the handedness of the  $\alpha$  quartz sample; i.e., if we start with an  $\alpha_1$  (or right-handed) quartz sample, we always obtain the same shape, which is different than the shape that results from compressing an  $\alpha_2$  (or left-handed) sample. We would therefore classify the transition as coelastic, since the relevant ergodicity breaking had already occurred in  $\alpha$ -quartz. Also, as one may infer from the structure analysis presented further below, there is no obvious group-subgroup relationship be-

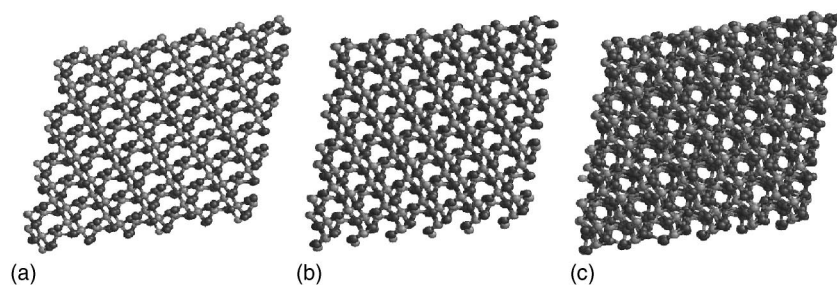


FIG. 2. Snapshots of (a)  $\delta$ -quartz ( $P=0$  GPa), (b) quartz II (25 GPa), and (c) quartz  $\text{II}_m$  (50 GPa). Light and dark atoms reflect, respectively, Si and O atoms.

tween the two phases. This certainly allows for the possibility that the phase transformation is coelastic.

The transition from  $\alpha$ -quartz to quartz II appears to be irreversible. On reducing the pressure, a transition into  $\alpha$ -quartz does not take place. Instead, a new phase is formed upon decompression at  $P_{\text{II-}\delta} \approx 5$  GPa, which we call  $\delta$ -quartz. The new  $\delta$ -quartz has structural similarity with  $\alpha$ -quartz, even though its space group  $C2$  is identical to that of quartz II. Both structures are formed from tetracoordinated Si—O network. The quartz II is a severely sheared form of  $\delta$ -quartz. Both transitions  $\text{I} \rightarrow \text{II}$  and  $\delta \leftrightarrow \text{II}$  are accompanied by dramatic changes in volume, which clearly points to a discontinuous phase transformation in both cases. The  $\text{II-}\delta$  transition exhibits distinct hysteresis effects.

Despite the quantitative difference between the BKS and the *ab initio* equation of state, both methods agree qualitatively. The topology of the equation of state diagram is produced correctly by BKS. While the density of  $\delta$ -quartz at ambient conditions is underestimated by about 10%, the (spinodal) transition pressures agree almost perfectly well with the *ab initio* values. Previously, the BKS-based prediction of a five-coordinated silica polymorph<sup>30</sup> had also been supported by *ab initio* calculations.<sup>31</sup> We therefore believe that BKS may correctly reproduce the qualitative features of the transitions of interest. It should be noted that we did not check for mechanical and dynamical stabilities of the *ab initio*—predicted structures. First-principles calculations of the elastic constants and phonon band structures are quite elaborate for systems with very low symmetry and beyond the feasibility of the present study.

Additional calculations were performed at even higher pressures. Their results are not included in Fig. 1. When  $P$  is increased *slowly* above 30 GPa, both molecular dynamics and *ab initio* calculations suggest a transition into a much-densified, disordered state. We conclude that quartz II becomes unstable at that point and that there is no obvious pathway from quartz II to another crystalline phase. However, when we compress a large simulation cell in molecular dynamics to very large pressures—i.e.,  $P=50$  GPa—a yet different crystalline phase (which we call quartz  $\text{II}_m$ ) is obtained. When decompressed adiabatically, quartz  $\text{II}_m$  remains stable down to 30 GPa, where it transforms back into quartz II. At that transition, only a small volume change of approximately 0.5% is observed. If the quartz  $\text{II}_m$  results were included into Fig. 1, the additional data would appear as an extension of the quartz II curve. Finally, we wish to comment that we do not believe that BKS potential is reliable for the extreme pressures necessary to produce quartz  $\text{II}_m$ . But we believe that the effect of the pressure-induced incommensu-

rate phase is an interesting effect in its own right without relating to an existing material.

## B. Structure and stability

All three post-quartz phases show structural similarity. Snapshots of the BKS calculations are shown in Fig. 2. One difference between  $\delta$ -quartz and quartz II is that the two oxygen atoms in the open spaces move on top of each other in the latter phase. The quartz  $\text{II}_m$  phase seems to be a modulated version of quartz II. The apparent disorder in the quartz  $\text{II}_m$  snapshot is frozen in at room temperature on the time scale of the simulation. We interpret this as a probably incommensurate modulation of the lattice, which is pinned. This seeming disorder is thus different from that in  $\beta$ -quartz (the high-temperature version of quartz I), where time-averaged structure and instantaneous structure can be distinguished fairly easily.<sup>13</sup> The long wavelength associated with the lattice modulation makes it presently unfeasible for *ab initio* methods to tackle the stability of quartz  $\text{II}_m$ . As mentioned above, we consider the effect related to quartz- $\text{II}_m$  an interesting effect of the BKS potential rather than a phase transformation in real  $\text{SiO}_2$ . Despite their structural similarities, all phase transformations between the three (BKS) post-quartz phases are discontinuous (first order).

Overall, *ab initio* and BKS results agree very well with one important exception: BKS  $\delta$ -quartz turns out to have lower (free) enthalpy than  $\alpha$ -quartz above 4 GPa, whereas *ab initio* values for the enthalpy do not favor  $\delta$ - over  $\alpha$ -quartz at any pressure within the range where both phases are metastable. Thus, there is a bias in BKS that certainly favors the sheared post-quartz structure. Despite this discrepancy, we are confident that a mechanical stability analysis for the BKS potential is meaningful, because the values for the pressures at which the spinodals are found agree almost perfectly between BKS and *ab initio* calculations and experiment. This includes the amorphization of quartz II, which occurs when  $P$  is increased *slowly* above 30 GPa.

As mentioned in the Introduction, Kingma *et al.*<sup>4</sup> and Haines *et al.*<sup>6</sup> arrived at quite different diffraction patterns for the metastable 25 GPa quartz polymorph. Analyzing the x-ray scattering intensity  $S(Q)$  that one can obtain from our simulations favors the earlier results by Kingma *et al.* Some of the nonquartz entities in their diffraction patterns (which the authors attributed speculatively to the pressure mediating neon) occur at places where we find peaks due to quartz II; see Fig. 3. We thus believe that our simulation reproduce the configurations obtained experimentally by Kingma *et al.* rather than by Haines *et al.*

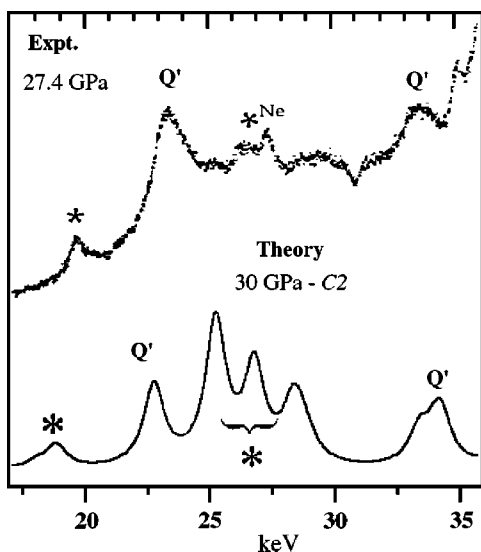


FIG. 3. X-ray diffraction intensity as measured experimentally (Ref. 4) and as obtained from simulations.

One could speculate that the difference between the structures observed by Kingma *et al.*<sup>4</sup> and Haines *et al.*<sup>6</sup> is that in Ref. 6 the experiment was performed under good hydrostatic conditions due to the use of helium as the pressure medium. However, no medium was used in the earlier experiments of Ref. 4. In the latter case, the structural transformation is likely to be kinetic rather than truly thermodynamic (within the phases accessible through displacive transformations). The MD calculations may be more closely related to kinetic transformations rather than to thermodynamic transformations. Unfortunately, it is difficult to ascertain this speculation within MD.

Further confidence in the correctness of the phase transformation was obtained by using a different, more realistic potential energy surface: namely, the fluctuating dipole potential by TS.<sup>17</sup> While the transition pressure was higher for TS than for BKS—namely, at 28 GPa—the same SiO<sub>2</sub> polymorph was obtained in TS as with BKS. The decompression scenario with TS is slightly different than that in BKS; however, most features remain similar. In particular, the I→II transition remains coelastic and irreversible. Upon decreasing pressure, the system undergoes a reversible, discontinuous phase transformation into a structure that is again a decompressed version of the quartz II structure. This occurs in the TS potential at a pressure slightly above 20 GPa. We also add that the TS quartz II (to be precise its decompressed phase) did not remain stable all the way down to 0 GPa, but reverted very slowly to  $\alpha$  quartz at about 7 GPa. Thus, even though the TS potential had certainly a much smaller bias towards the sheared post-quartz structures than the BKS potential, qualitatively similar behavior was found. More details will be reported on the TS potential elsewhere.<sup>25</sup>

The space group of  $\delta$ -quartz and quartz II is C2 (Ref. 33). It is interesting to note that the unit cell does not triple in the  $z$  direction, even though  $\alpha$ -quartz does become unstable near the  $K$  point of the Brillouin zone.<sup>2</sup> The number of atoms per unit cell (9) even turns out to be unchanged. We conclude that the quartz II phase does not follow the Landau scheme

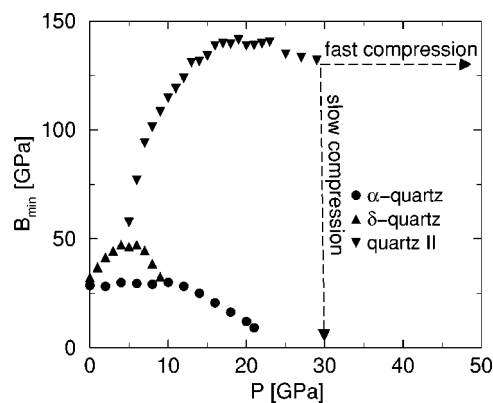


FIG. 4. Minimum eigenvalue  $\lambda$  of matrix of stiffness coefficients  $B$  as a function of pressure  $p$ .

and note that the final structure does not have to be commensurate with the soft mode, because the transition is not second order.

In order to address the mechanical stability of the various phases, we analyzed the Born stability criterion (BSC) at finite pressures. As discussed in Refs. 9, 11, and 12, the correct BSC at nonzero temperatures is based on stiffness or Birch coefficients  $B_{\alpha\beta}$  rather than on elastic constants: In order for a solid to be mechanically stable, all eigenvalues of the  $B$  matrix must be positive. The Birch coefficients  $B$  result as second derivatives of the free energy  $\mathcal{F}$  with respect to Lagrangian strain, while elastic constants  $C_{\alpha\beta}$  are defined as the second derivative of  $\mathcal{F}$  with respect to the Eulerian strain. Both definitions coincide only at zero-external pressure.

Figure 4 shows the minimum eigenvalues of  $B$  for  $\alpha$ -quartz and the three post-quartz polymorphs. Only  $\alpha$ -quartz becomes soft (i.e.,  $B_{\min} < 5$  GPa) near the transition, even though, strictly speaking, it does not soften completely in the thermodynamically (meta) stable region.<sup>2,9,32</sup> While the absolute values of  $B_{\min}$  remain large in the other phases, the slopes of  $B_{\min}$  become large near the  $\delta \leftrightarrow$  II transformation. This is indicative of a coupling of the modes that drive the transition to the long-wavelength modes. The arrows “fast” and “slow” in Fig. 4 indicate that in one case the externally applied pressure is abruptly increased from 30 GPa to 50 GPa. The simulation cell can quickly respond to these dramatic changes provided that its inertia is chosen sufficiently small. In a slow compression simulation,  $p$  is increased incrementally by 2 GPa. After each pressure change, the system is equilibrated for a few 10 000 MD steps so that the pressure change can be considered essentially adiabatic as long as the structural rearrangements can be classified as displacive and no phase transition occurs. For each pressure, the box geometry would be given sufficient time to equilibrate provided that no lattice reconstruction occurred.

The arrow labeled “slow compression” also reflects a situation in which a large value for the simulation cell’s effective mass is employed. This choice prevents the volume from finding quickly (or getting stuck at) the next available minimum. The system densifies very strongly and starts “flowing,” which results in  $B_{\min}=0$ . If, however, the simulation cell’s inertia is chosen sufficiently small, the volume change

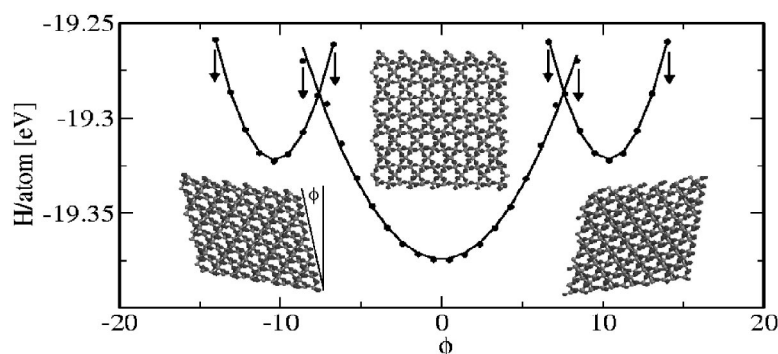


FIG. 5. Energy per atom as a function of shear angle  $\Phi$ . The left- and right-handed BKS  $\delta$ -quartz polymorphs can be transformed into one another by going through an intermittent  $\alpha$ -quartz phase. The crystals amorphinize irreversibly at the arrows marked **1** and **1'**.

can occur concurrently with the structural, atomic rearrangements and it is possible to lock into a less dense crystalline state.

### C. Ferroelasticity of quartz II and $\delta$ -quartz

For a crystal to be called ferroelastic, one might want to require that it must be possible to switch elastically (i.e., without bond breaking) between different, however, energetically equivalent stable shapes. In the simulations of quartz II and  $\delta$ -quartz, we attempted such a switch by confining the angle  $\Phi$ , denoted in Fig. 5 and by evolving the system under constant stress otherwise. From one simulation to the next,  $\Phi$  was moved by a value close to  $1^\circ$  and the system was given sufficient time to find the next available energy minimum. The result of such a set of simulation at zero external stress is shown in Fig. 5.

The stability of BKS  $\delta$ -quartz is approximately in the range of  $6^\circ \leq |\Phi| \leq 14^\circ$ . Upon decreasing  $|\Phi|$  from the stability region,  $\delta$ -quartz converts into  $\alpha$ -quartz at  $|\Phi| \approx 6^\circ$  with—as far as we can tell—random handedness. Upon increasing  $|\Phi|$ , the crystalline structure amorphinizes at  $|\Phi| \approx 14^\circ$  and no recrystallization occurs on the time scale of the simulation if the constraint of fixed  $\Phi$  is released.

Similar calculations were conducted at different pressures and different temperatures.  $\alpha$ -quartz occurs as an intermittent phase even at  $p=5$  GPa, when the BKS potential (wrongly) predicts  $\delta$ -quartz to be energetically favorable to  $\alpha$ -quartz at constant strain. Conversely, quartz II cannot be switched from one state into the other in our simulations without becoming unstable when the stress is kept fixed except for the stress component controlling the tilt angle  $\Phi$ . At large pressures (25 GPa), quartz II amorphinizes under shear while attempting to invert the strain. At lower pressures (13 GPa), the behavior is more complex: Quartz II seems to convert into a yet different polymorph under shear; however, this phase is unstable against thermal noise once the condition of fixed order parameter is released. Sometimes, this new polymorph reverts back to the old quartz II configuration. Thus, while there is a shape change of the elementary cell of right-handed and left-handed quartz II, there is no obvious way how to switch between the two mirror images of quartz II directly without passing through two intermittent  $\delta$ -quartz phases and one  $\alpha$ -quartz phase. Nevertheless, since it seems possible to switch quartz II one might classify it as ferroelastic.

## IV. CONCLUSIONS

In conclusion, the present study shows that the pressure-induced transition from (BKS)  $\alpha$ -quartz to the post-quartz phases is irreversible, as long as we consider only isotropic stresses. We identify three post-quartz phases, which we labeled  $\delta$ -quartz, quartz II, and quartz II<sub>m</sub>. They can be transformed into one another reversibly by changing the (isotropic) pressure. There is, however, the restriction that quartz II has to be compressed rather quickly from its stability region to pressures close to 45 GPa, in order to circumnavigate a collapse into a phase with even higher density than that of quartz II<sub>m</sub>. Despite this restriction, we obtain the same post-quartz phase at ambient conditions if we decompress (adiabatically) quartz II from  $P=25$  GPa or quartz II<sub>m</sub> from  $P=50$  GPa.

We also found an ergodicity breaking related to the shape of the post-quartz crystals and in this sense the post-quartz phases can be labeled as ferroelastic. However, the shape of the post-quartz crystals is predetermined by the handedness of  $\alpha$ -quartz. Thus the pressure-induced transformation to and between the post-quartz phases are not ferroelastic. Even worse, the post-quartz phases might not be ferroelastic in the sense that an *elastic* force can be applied such that we switch between directly different, but symmetrically equivalent states. Preliminary simulations suggest the following picture: If we try to convert  $\delta_1$ -quartz to  $\delta_2$ -quartz by applying a *nonisotropic* external stress, the crystal becomes unstable and converts back to  $\alpha$ -quartz. Thus, in order to “switch” quartz II, it will probably be required to pass through a decompressed quartz II structure that can be switched by passing through an intermittent  $\alpha$  quartz phase.

Using more realistic model potentials such as the TS potential,<sup>17</sup> yields similar results. TS  $\alpha$ -quartz converts into the same high-pressure polymorphs as BKS  $\alpha$ -quartz, albeit at slightly higher pressure. Upon decompression, an intermittent decompressed quartz II phase is identified. The largest difference between the TS and BKS potentials is that the BKS potential favors much more strongly sheared tetrahedral SiO<sub>4</sub> units than the TS potential. As a consequence, the TS-decompressed quartz II phase becomes unstable at 7 GPa and reverts to  $\alpha$ -quartz. More details will be presented in a comparison of the reliability of BKS, TS, and other model potentials.<sup>25</sup>

## ACKNOWLEDGMENTS

M.H.M. thanks Kurt Binder for useful discussions. J.T. and M.H.M. gratefully acknowledge support from NSERC.

C.C. and M.H.M. gratefully acknowledge support from Sharcnet. P.S. and D.H. received support from the BMBF through Grant No. 03N6015 and from the Materialwissenschaftliche Forschungszentrum Rheinland-Pfalz.

- 
- <sup>1</sup>J. S. Tse and D. D. Klug, *Phys. Rev. Lett.* **67**, 3559 (1991).  
<sup>2</sup>N. Binggeli and J. R. Chelikowsky, *Phys. Rev. Lett.* **69**, 2220 (1992); **71**, 2675 (1993).  
<sup>3</sup>K. J. Kingma, *et al.*, *Science* **259**, 666 (1993).  
<sup>4</sup>K. J. Kingma, R. J. Hemley, H. K. Mao, and D. R. Veblen, *Phys. Rev. Lett.* **70**, 3927 (1993).  
<sup>5</sup>J. S. Tse, *et al.*, *Phys. Rev. B* **56**, 10 878 (1997). Full *ab initio* geometry optimization of the reported *P1* structure relaxed to the same *C2* phase described here.  
<sup>6</sup>J. Haines, J. M. Léger, F. Gorelli, and M. Hanfland, *Phys. Rev. Lett.* **87**, 155503 (2001).  
<sup>7</sup>A. P. Mirgorodsky *et al.*, *Phys. Rev. B* **52**, 3993 (1995).  
<sup>8</sup>E. Gregoryanz, R. J. Hemley, H. K. Mao, and P. Gillet, *Phys. Rev. Lett.* **84**, 3117 (2000).  
<sup>9</sup>M. H. Müser and P. Schöffel, *Phys. Rev. Lett.* **90**, 079701 (2003).  
<sup>10</sup>E. Gregoryanz, R. J. Hemley, H. K. Mao, R. E. Choen, and P. Gillet, *Phys. Rev. Lett.* **90**, 079702 (2003).  
<sup>11</sup>D. C. Wallace, in *Solid State Physics*, edited by H. Ehrenreich, F. Seitz, and D. Turnbull (Academic Press, New York, 1971), Vol. 25; *Thermodynamics of Crystals* (Wiley, New York, 1972).  
<sup>12</sup>J. Wang, S. Yip, S. R. Phillpot, and D. Wolf, *Phys. Rev. Lett.* **71**, 4182 (1993).  
<sup>13</sup>M. H. Müser, in *Particle Scattering, X-Ray Diffraction, and Microstructure of Solids and Liquids*, Lecture Notes in Physics, Vol. 610, edited by K. A. Gernoth and M. L. Ristig (Springer, Berlin, 2003).  
<sup>14</sup>E. K. H. Salje, *Phase Transitions in Ferroelastic and Co-elastic Crystals* (Cambridge University Press, New York, 1990).  
<sup>15</sup>P. Schöffel, Diploma thesis, University of Mainz, 2000.  
<sup>16</sup>B. W. H. van Beest, G. J. Kramer, and R. A. van Santen, *Phys. Rev. Lett.* **64**, 1955 (1990).  
<sup>17</sup>P. Tangney and S. Scandolo, *J. Chem. Phys.* **117**, 8898 (2002).  
<sup>18</sup>S. Tsuneyuki, M. Tsukada, H. Aoki, and Y. Matsui, *Phys. Rev. Lett.* **61**, 869 (1988).  
<sup>19</sup>P. Vashishta, R. K. Kalia, J. P. Rino, and I. Ebbsjo, *Phys. Rev. B* **41**, 12 197 (1990).  
<sup>20</sup>J. S. Tse and D. D. Klug, *J. Chem. Phys.* **95**, 9176 (1991).  
<sup>21</sup>M. H. Müser and K. Binder, *Phys. Chem. Miner.* **28**, 746 (2001).  
<sup>22</sup>M. H. Müser, *J. Chem. Phys.* **114**, 6364 (2002).  
<sup>23</sup>J. Horbach, W. Kob, and K. Binder, *J. Phys. Chem. B* **103**, 4104 (1999); *Eur. Phys. J. B* **19**, 531 (2001).  
<sup>24</sup>M. Parrinello and A. Rahman, *J. Chem. Phys.* **76**, 2662 (1982).  
<sup>25</sup>D. Herzbach, K. Binder, and M. H. Müser (unpublished).  
<sup>26</sup>G. Kresse and J. Furthmüller, *Phys. Rev. B* **54**, 11 169 (1996); *Comput. Mater. Sci.* **6**, 15 (1996).  
<sup>27</sup>D. Vanderbilt, *Phys. Rev. B* **41**, 7892 (1990); G. Kresse and D. Joubert, *ibid.* **59**, 1758 (1999).  
<sup>28</sup>N. Binggeli, J. R. Chelikowsky, and R. M. Wentzcovitch, *Phys. Rev. B* **49**, 9336 (1994).  
<sup>29</sup>M. S. Somayazulu, S. M. Sharma, and S. K. Sikka, *Phys. Rev. Lett.* **73**, 98 (1994).  
<sup>30</sup>J. Badro, J.-L. Barrat, and P. Gillet, *Phys. Rev. Lett.* **76**, 772 (1996).  
<sup>31</sup>J. Badro *et al.*, *Phys. Rev. B* **56**, 5797 (1997).  
<sup>32</sup>J. S. Tse, D. D. Klug, and Y. Le Page, *Phys. Rev. B* **46**, 5933 (1992).  
<sup>33</sup>The unit cell parameters for quartz II at 21 GPa are (*a*, *b*, *c*, and  $\beta$ =8.417 Å, 3.459 Å, 5.221 Å, and 108.8°) with atomic coordinates: Si(1) -0.5000, 0.0506, 0.0000; Si(2) -0.3225, 0.8073, -0.3809; O(1) -0.5048, -0.1868, -0.7251; O(2) -0.6863, 0.3058, -0.5751; O(3) -0.3330, 0.3016, -0.9156. For  $\delta$ -quartz at 3 GPa, the cell parameters are 9.131 Å, 3.630 Å, 5.668 Å, and 92.75° and Si(1) -0.5000, 0.0551, 0.0000; Si(2) -0.2669, 0.8000, -0.3193; O(1) -0.5703, -0.1802, -0.7869; O(2) -0.2385, 0.8088, -0.6148; O(3) -0.3676, 0.3011, -0.8789.